Atmospheric Environment 203 (2019) 141–152

Contents lists available at ScienceDirect

Atmospheric Environment

journal homepage: www.elsevier.com/locate/atmosenv

Trends in remote $PM_{2.5}$ residual mass across the United States: Implications for aerosol mass reconstruction in the IMPROVE network

J.L. Hand[a,*], A.J. Prenni[b], B.A. Schichtel[b], W.C. Malm[a], J.C. Chow[c]

[a] Cooperative Institute for Research in the Atmosphere, Colorado State University, Fort Collins, CO, 80523, USA
[b] National Park Service, Air Resources Division, Lakewood, CO, 80235, USA
[c] Division of Atmospheric Sciences, Desert Research Institute, Reno, NV, 89512, USA

GRAPHICAL ABSTRACT

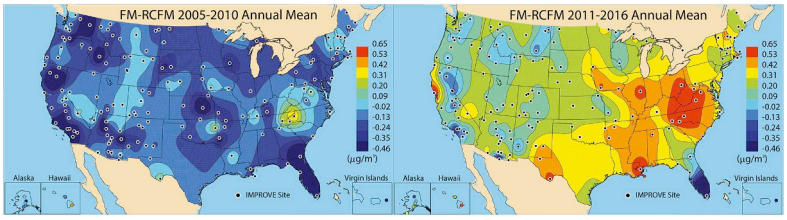

ARTICLE INFO

Keywords:
Reconstructed mass
$PM_{2.5}$ mass
Remote aerosols
IMPROVE network

ABSTRACT

The Interagency Monitoring of Protected Visual Environments (IMPROVE) network collects aerosol samples for gravimetric and composition analysis in support of the Environmental Protection Agency's Regional Haze Rule and for long-term trend studies and model evaluations. Reconstructing $PM_{2.5}$ mass or extinction from composition measurements requires assumptions of the molecular form of the individual species assumed to compose the bulk of $PM_{2.5}$ mass. The IMPROVE reconstruction algorithm includes sulfate as ammonium sulfate, nitrate as ammonium nitrate, organic mass calculated with an assumed organic carbon (OC) to organic mass (OM) multiplier (OM/OC) of 1.8, elemental carbon, fine dust assuming common mineral oxides in soil, and sea salt calculated from chloride. Comparisons of reconstructed fine mass (RCFM) to $PM_{2.5}$ gravimetric fine mass (FM) provide a check on these assumptions as well as help identify possible biases in gravimetric or speciated measurements. Significant changes in aerosol concentration and composition have occurred over time, leading to decreased FM across the United States. However, within the IMPROVE network, annual mean FM and RCFM have decreased at different rates from 2005 through 2016 (−29% versus −43%, respectively), causing the network median residuals (FM − RCFM) to increase by $0.49\,\mu g\,m^{-3}$ over the 12-year period. The residual shifted from mostly negative before 2011 to mostly positive after 2011, with a strong summer peak. A multiple linear regression analysis indicated that FM biases increased due to the presence of particle-bound water (PBW) after 2011, associated with increased laboratory relative humidity during weighing. Results also suggested that the OM/OC ratio increased across the network after 2011, unrelated to the influence of PBW. While temporal behavior in the OM/OC ratio was similar across the network and for all seasons, values were highest in the East and during summer. Fine dust also appeared to be underestimated by ~20%. Identifying the source of the trends in the FM residual is essential for accurately estimating contributions by individual species to RCFM and visibility degradation.

* Corresponding author. CIRA, 1375 Campus Delivery, Colorado State University, Fort Collins, CO, 80523, USA.
E-mail address: jlhand@colostate.edu (J.L. Hand).

https://doi.org/10.1016/j.atmosenv.2019.01.049
Received 5 November 2018; Received in revised form 18 January 2019; Accepted 19 January 2019
Available online 31 January 2019
1352-2310/

1. Introduction

Bulk $PM_{2.5}$ (particles with aerodynamic diameters less than 2.5 μm) gravimetric mass measurements are made as part of the Environmental Protection Agency's (EPA) Federal Reference Method (FRM) network to assess compliance with National Ambient Air Quality Standards (NAAQS). Complementing the FRM network, speciated measurements of $PM_{2.5}$ aerosol mass composition are important for accurately assessing the sources, transport, atmospheric processing and transformation, health impacts, radiative impacts (e.g., visibility and radiative forcing), and cloud processing because these impacts often depend on aerosol physical and chemical properties. Studying temporal and spatial trends in speciated mass is important for understanding impacts of pollutant emissions (e.g., Hand et al., 2012a,b; Blanchard et al., 2013, 2016; Attwood et al., 2014; Hidy et al., 2014; Prenni et al., 2016) and for designing appropriate pollutant mitigation strategies. Networks such as the Interagency Monitoring of Protected Visual Environments (IMPROVE) (Malm et al., 1994) and EPA's Chemical Speciation Network (CSN) (Solomon et al., 2014) have been measuring speciated aerosol mass for decades at hundreds of remote and urban sites, respectively. While the networks exist for different purposes, they have similar monitoring and analysis methods for characterizing speciated and bulk $PM_{2.5}$ mass.

Monitoring from the IMPROVE network supports the EPA's Regional Haze Rule (RHR) which tracks trends in visibility degradation at class I (visibility-protected) areas in the United States, with the goal to return visibility to natural conditions by 2064 (U.S. EPA, 2003). The IMPROVE algorithms for reconstructing mass and aerosol light extinction were originally developed by Malm et al. (1994) to account for individual species' contributions to $PM_{2.5}$ mass and total aerosol extinction. The identification of possible biases in light extinction estimates (Lowenthal and Kumar, 2003) led to a revision of the original IMPROVE reconstructed mass and extinction algorithms (Malm and Hand, 2007; Pitchford et al., 2007) that were adopted as part of the RHR guidelines. The form of the new (or "second") IMPROVE mass reconstruction algorithm is shown in equation (1):

$$RCFM = AS + AN + OM + EC + Dust + SS \quad (1)$$

where reconstructed fine mass (RCFM) is the sum of mass concentrations associated with major components of $PM_{2.5}$ mass. Ammonium sulfate (AS) is calculated with sulfate ion data ($AS = 1.375 \times SO_4^{2-}$) and ammonium nitrate (AN) is calculated using nitrate ion data ($AN = 1.29 \times NO_3^-$). Carbonaceous aerosols are included as organic matter (OM), calculated from organic carbon (OC) using an OM/OC ratio of 1.8 (Malm and Hand, 2007), and elemental carbon (EC). Fine dust is calculated assuming normal oxides of typically occurring soil species ($Dust = 2.20 \times Al + 2.49 \times Si + 1.63 \times Ca + 2.42 \times Fe + 1.94 \times Ti$), including aluminum (Al), silicon (Si), calcium (Ca), iron (Fe), and titanium (Ti). Sea salt (SS) is calculated with chloride ion data ($SS = 1.8 \times Cl^-$; White, 2008). This equation differs from the "original" IMPROVE algorithm (Malm et al., 1994) in that the OM/OC increase from 1.4 to 1.8 and SS is included. While this specific approach was adopted by the EPA for the RHR guidelines, within the larger community many different equations and assumptions have been used to reconstruct fine mass, as reviewed by Chow et al. (2015a).

Dramatic reductions in speciated aerosol mass (e.g., SO_4^{2-} and OC) observed over the last decade, as well as changing emissions (i.e., reductions in anthropogenic emissions alongside increased natural emissions such as wildfire smoke and dust), have led to changes in aerosol composition across the United States (e.g., Blanchard et al., 2013, 2016; Hand et al., 2017; Malm et al., 2017; Chan et al., 2018; Kaku et al., 2018; Shah et al., 2018). In addition, operation of a long-term network such as IMPROVE requires sampling, analysis, and hardware upgrades over time (e.g., Chow et al., 2015b; Hyslop et al., 2015). Potential effects of all of these changes can be seen in the comparison of the IMPROVE annual mean $PM_{2.5}$ mass residual. The fine mass residual is defined as the difference in $PM_{2.5}$ gravimetric fine mass measurements (also referred to as FM) and RCFM (residual = FM − RCFM). The fine mass residual for 2005–2010 and 2011–2016 are compared in Fig. 1a and b, respectively. All available IMPROVE sites from both periods are shown as dots on the maps. Details regarding data in these maps are provided in Section 2.

Annual mean residuals have shifted dramatically between the two periods. The RCFM algorithm (equation (1)) overestimated FM (negative residual) across the network during the first period (Fig. 1a), whereas during the later time period (Fig. 1b) the algorithm appeared to underestimate FM across the country. This change in the residual suggests that the reconstruction algorithm has increasingly underestimated FM over time, that biases in measured FM have increased, that biases in individual species have changed, or a combination of any or all of these.

The assumptions used in the reconstruction algorithm in equation (1) are the foundations for estimating visibility impacts as part of the RHR and were last evaluated in 2007 (Malm and Hand, 2007; Pitchford et al., 2007). Given the significant increase in the residual shown in Fig. 1, it is crucial to understand whether these changes are due to assumptions applied in the reconstruction algorithm, changes in sampling or analytical biases, or recent trends in aerosol composition. Investigations into these various issues form the basis of this manuscript. In Section 2, a data description and summary of network sampling and analytical changes are provided. Assumptions in the reconstruction algorithm are investigated in Section 3. Implications for these combined changes on the residual are discussed in Section 4.

2. Data and methods

The IMPROVE network has been operating since 1988 with the purpose of monitoring visibility conditions at class I areas throughout the United States. To this end, IMPROVE uses four separate modules to collect samples for speciated $PM_{2.5}$ analysis and gravimetric $PM_{2.5}$ and

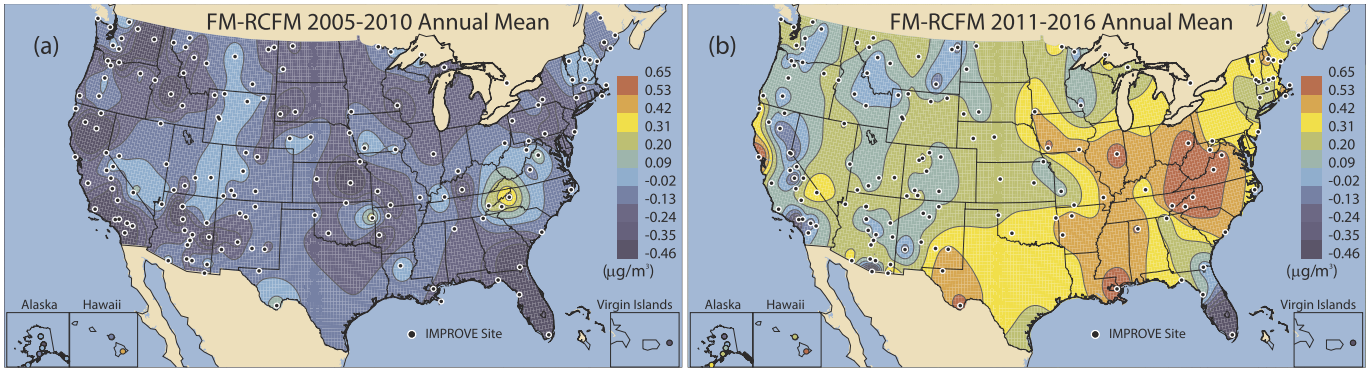

Fig. 1. IMPROVE annual mean fine mass residual (FM − RCFM, μg m^{-3}) for (a) 2005–2010 and (b) 2011–2016. Dots correspond to IMPROVE sites.

PM_{10} (particles with aerodynamic diameters less than 10 μm) bulk mass measurements in remote and rural regions (Malm et al., 1994). Samples are collected for 24 h every third day and reported at local conditions (not corrected to standard pressure and temperature) at approximately 160 sites currently operating. $PM_{2.5}$ anions (SO_4^{2-}, NO_3^-, and Cl^-) are analyzed from nylon filters using ion chromatography and are blank corrected (Zhang, 2017). $PM_{2.5}$ carbonaceous aerosols (OC and EC) are analyzed from quartz filters using a thermal optical reflectance (TOR) protocol (Chow et al., 2007). OC and EC thermal fractions are reported, and each fraction is corrected for a positive additive artifact (Watson et al., 2009; Chow et al., 2010) but not a multiplicative artifact (Malm et al., 2011). Filters are not shipped under controlled temperature conditions (Dillner et al., 2009). $PM_{2.5}$ trace elements are analyzed from Teflon filters using X-ray fluorescence (XRF). $PM_{2.5}$ gravimetric mass is determined from the same Teflon filters that are used for XRF analysis. PM_{10} gravimetric mass is determined from a separate Teflon filter, downstream of the PM_{10} inlet.

IMPROVE data were downloaded from the Federal Land Manager Environmental Database (FED; http://views.cira.colostate.edu/fed/; data downloaded on 9 April 2018). Daily data, uncertainties, and minimum detection limits (MDL) are also available on the FED website. Additional details, such as site location and monitoring and analytical details are reported by Hand et al. (2011) and on the IMPROVE website (http://vista.cira.colostate.edu/improve/). Data were used as reported, except for elemental XRF species. Before 2011 XRF data below MDLs were replaced by 0.5 × MDL; after 2011 values were used as reported. An explanation of this change is provided later in this section. Data shown in Fig. 1 were interpolated using an ordinary kriging algorithm (Isaaks and Mohan Srivastava, 1989) to provide spatial patterns to guide the eye. Trends were calculated using Theil regression (Theil, 1950), and significance levels were determined with Kendall tau statistics.

The species used in this study include SO_4^{2-}, NO_3^-, Cl^-, OC, EC, XRF species including sulfur (S), chlorine (Cl), Al, Si, Ca, Fe, and Ti, and gravimetric $PM_{2.5}$ mass (FM). Changes in sampling protocol, analytical techniques, or data issues related to these species are described in this section. These changes are regularly documented through IMPROVE data advisories (http://vista.cira.colostate.edu/Improve/data-advisories/).

As stated earlier, SO_4^{2-} is used to calculate AS, and SO_4^{2-} analyses have remained fairly consistent over time. However, the methods to determine analytic detection limits and uncertainties were modified for data reported from 2005 to present (Cheng, 2015). Missing SO_4^{2-} data were replaced with 3 × S. From 2003 to 2008, discontinuities in XRF-derived S concentrations corresponded to recalibrations of the XRF system. A new calibration protocol was applied to the 2007–2008 data (White, 2009a). In 2011 the network shifted to a PANalytical XRF system, which reduced MDLs for several species. Therefore, before 2011, S values below the MDL were replaced with 0.5 × MDL; starting in 2011, S values are used as reported. Calculating AS with only S did not change the results in this study.

AN concentrations are calculated using NO_3^- in equation (1). NO_3^- concentrations during winter months at many IMPROVE sites were below historical levels for 1996–1997 and 1999–2000 for unknown causes. Data since mid-2000 are considered to be valid (McDade, 2007).

SS concentrations are determined using Cl^-. Cl^- concentrations at inland (noncoastal) sites are generally low due to ion replacement (White, 2008; Hand et al., 2012a) and lack of proximity to sources. From 2000 through 2003, concentrations at inland sites were often negative and associated with high Cl^- backgrounds on the filters (White, 2009b, 2017). Cl^- values were replaced with Cl from XRF if Cl^- values were missing.

Carbon measurements have experienced several changes over time. Samples collected on or after 1 January 2005 were analyzed with new TOR hardware and a new temperature protocol (Chow et al., 2007). Minor differences in the EC to total carbon (OC + EC) ratios were identified between the old and new hardware (before and after 2005) (White, 2007). Analysis of EC trends by Chen et al. (2012) suggested minor impacts to EC; however, trends in independent filter reflectance data corroborated EC trends from 2000 through 2009. Hardware degradation (Chow et al., 2015b) also resulted in new TOR hardware and analysis methods for samples collected and analyzed beginning in 2016.

OC carbon fraction concentrations are corrected to account for a positive additive artifact due to gas-phase adsorption of OC onto quartz filters (Watson et al., 2009; Chow et al., 2010). Earlier artifact corrections on OC fractions used monthly median OC fractions from backup filters located downstream of the primary filter at a handful of sites. The revised correction instead uses monthly median blank filters. Blank filters are loaded in the filter cassettes and remain in the sampler for the same length of time but have no air pulled through them. The new artifact corrections were applied to data from 2005 onward, and data downloaded after May 2015 reflect these changes (Dillner, 2015). In addition, MDLs and uncertainty calculations were modified.

Several changes in XRF analytical techniques have occurred over time, and the effects of these changes on elemental species have been reported by Hyslop et al. (2015). The 2011 switch to the PANalytical XRF system also resolved issues related to undetected Al with concentrations above the MDL (White, 2006a). In addition, field blank selection criteria for calculating blank subtractions were modified for 2011 and later (Cheng, 2015).

Starting in December 2001, interference of Si and Al by S in the XRF measurement might have resulted in erroneous Si and Al concentrations when S ≫ Si (White, 2006a,b). The screening approach by Indresand and Dillner (2012) suggested that Si was over-reported, and Al had high uncertainty when S/Fe > 8. No S interference was observed for samples corresponding to S/Fe < 8. These errors are expected to affect 50% of the data from 1 December 2001 through 31 December 2010. These issues were resolved in 2011 with the switch to the PANalytical XRF system.

IMPROVE FM measurements do not meet EPA requirements for the FRM measurement (U.S. EPA, 2016), which limits laboratory relative humidity (RH) to 30–40% and temperature to 20–23 °C during weighing and the length of time between sample collection and weighing (10 days if not stored under 25 °C). Prior to 2011, periodic laboratory RH measurements suggested that RH was typically below 50%; however, a laboratory relocation in 2011 resulted in unstable weighing conditions. Laboratory RH was not continuously recorded, but available data suggested that RH varied significantly during weighing and since 2011 exceeded 40% for almost half of the sample weighings, occasionally exceeding 60% (White, 2016). Thus, FM data from 2011 through 2016 were potentially subject to high RH conditions and likely contained particle-bound water (PBW).

To account for PBW directly, we calculated aerosol water content for every sample in the network. Hygroscopic growth curves were derived for AS, AN, SS, and OC individually using the Extended Aerosol Inorganic Model (E-AIM) thermodynamic model II (AS, AN) and model III (SS) (Wexler and Clegg, 2002; http://www.aim.env.uea.ac.uk/aim/aim.php; accessed 10 February 2017) at 298.15 K and for an RH range of 10–100% assuming no solids form (efflorescence branch). OC growth curves were calculated assuming a kappa of 0.1 (Prenni et al., 2007). Total water content for RH = 0–100% was calculated using the Zdanovskii-Stokes-Robinson (ZSR) approximation for each sample from every site from 2005 through 2016. Laboratory RH data were available for 2004, 2007 (winter and fall), 2008, 2009 (winter, spring), 2012 (fall, winter), and 2013–2016 (White, 2016). For periods with missing data, RH seasonal means from all data were assumed. Missing data from 2007 through 2009 were replaced by seasonal mean data from that same time period; missing data from 2011 to 2012 through 2016 were replaced by seasonal mean data from 2012 through 2016. A delay of several weeks between sample collection and weighing is common, so PBW was calculated according to the weighing date for each sample. Laboratory RH can vary within short time periods, so it is possible that

equilibrium on the filter was not established with the recorded RH when filters were weighed. PBW mass was subtracted from FM to determine a "dry" FM (FM_{dry}) for RH = 0%. PBW and FM_{dry} should be considered estimates given the many uncertainties associated with the calculation, including laboratory RH filter equilibrium, assumptions about the forms of hygroscopic species on the filter, and assumptions of RH when no records were available.

The FM residual is defined as the difference between measured FM and RCFM (FM − RCFM). RCFM was calculated using equation (1). If any of the species used in the reconstruction for a given sample was invalid, RCFM was considered invalid for that sample. The analysis was limited to data collected from 1 January 2005 to 31 December 2016 given the number of changes that occurred in the network prior to 2005. Annual mean residuals, such as those shown in Fig. 1, were calculated as the mean of daily residuals.

The assumptions applied in the RCFM algorithm can potentially bias the residual. For example, assumptions of fully neutralized AS could lead to higher RCFM relative to a more acidic form. In fact, recent field measurements suggest that especially in the East, SO_4^{2-} is in a more acidic form (Hidy et al., 2014; Kim et al., 2015; Lowenthal et al., 2015; Weber et al., 2016, Silvern et al., 2017). Assuming a form of ammonium bisulfate would lower the SO_4^{2-} contribution to RCFM by 15% (1.375/1.2). Nitrate could also exist in a different molecular form with crustal elements such as Ca or sodium (Na) (Lee et al., 2008; Allen et al., 2015), which could increase or decrease NO_3^- related mass by up to 10%. One of the largest uncertainties in the RCFM algorithm is the OM/OC ratio. The OM/OC ratio accounts for unmeasured species, such as hydrogen, oxygen, or other components (Turpin and Lim, 2001). Higher OM/OC values reflect a more aged secondary organic aerosol or biomass smoke (~2), whereas lower values (~1.4) are indicative of a less aged primary organic aerosol. The value of 1.8 used in equation (1) was derived from analysis of IMPROVE data from 1988 through 2003 by Malm and Hand (2007). Applying an inappropriate OM/OC value could bias the RCFM either low or high. SS can be calculated from other species associated with sea water (e.g., Lowenthal and Kumar, 2006; White, 2008) such as Na; however, Cl^- was used in equation (1) because Na is poorly quantified by XRF. However, SS as calculated by Cl^- could be underestimated because of Cl^- loss due to reactions on the filter (White, 2008) or in the atmosphere (Finlayson-Pitts, 2003). Finally, mineral dust as calculated by equation (1) assumes normal oxides of elements associated with soil and applies a correction factor to account for other compounds (Malm et al., 1994); earlier analysis by Malm and Hand (2007) suggested that dust may be underestimated by 20%, which would bias RCFM low relative to FM.

Biases in the FM measurement can also affect the residual. For example, NO_3^- volatilization from Teflon filters ($PM_{2.5}$ gravimetric measurement) can be significant, ranging from less than 10% in the cold season to 80% or more in the warm season (e.g., Hering and Cass, 1999; Chow et al., 2005), while NO_3^- loss from nylon filters is expected to be negligible. In addition, PBW associated with hygroscopic species on the Teflon filter can be significant depending on laboratory RH and can lead to higher FM relative to RCFM. Others have estimated the bias of PBW associated with hygroscopic species with a multiple linear regression (MLR) approach (e.g., Malm et al., 2011; see Section 3.2) or by measuring it directly (Rees et al., 2004; Perrino et al., 2016).

3. Results

3.1. Data

To understand the dramatic shift in the residual from mostly negative to mostly positive over time (Fig. 1), it is useful to examine trends in the species included in the reconstruction algorithm. Timelines from 2005 to 2016 of the residual and other species are shown as daily network medians in Fig. 2. Each point on the plot corresponds to a median of the data from all sites on that day. Discontinuities in the time series are indications of potential changes in the measurements or filter analyses that affect the entire network. FM and RCFM are plotted together in Fig. 2a, and the residual is shown in Fig. 2b. Measurement uncertainties in the residual are on the order of 0.1 $\mu g\,m^{-3}$ based on propagation of uncertainty estimates reported by Hyslop and White (2009). Major species contributing to RCFM are shown in Fig. 2c–h in the molecular forms assumed in the reconstruction algorithm (equation (1)) and in order of decreasing magnitude. Species with the highest concentrations are likely the main contributors to the residual. Vertical lines denote 1 January (solid) and 1 July (dashed) of each year. Light gray lines correspond to standard deviations.

FM, RCFM, and the residual all peaked in summer. The residual was typically negative in all seasons except in summers before 2011 and generally positive in all seasons after 2011, reaching 1 $\mu g\,m^{-3}$. Summer peaks in FM residual were also reported by Rees et al. (2004) in an urban environment. OM concentrations also peaked in summer and were the highest of any species (Fig. 2c). Primary sources of OM include combustion emissions, such as from biomass burning, which also peak in summer and early fall, especially in the western United States (Hand et al., 2013). Secondary organic aerosols formed through photochemical processes also peak in summer (e.g., Jimenez et al., 2009; Schichtel et al., 2017). The next highest concentrations were associated with AS (Fig. 2d), with summer peaks that reflected its formation processes related to photochemical activity. Both OM and AS have decreased over the last decade (Hand et al., 2012b, 2013; Blanchard et al., 2016; Ridley et al., 2018), and in the East their reductions were potentially related, due to the role of sulfate in secondary organic aerosol formation (Xu et al., 2015; Malm et al., 2017; Carlton et al., 2018). As shown in Fig. 2d, the seasonality in AS has decreased in recent years, as others have also reported (Kim et al., 2015; Chan et al., 2018), which could be related to availability of oxidants in winter leading to less of a decline during that season (Shah et al., 2018). Fine dust concentrations (Fig. 2e) peaked in spring and early summer (Hand et al., 2017) and have not experienced the same level of reduction as OM or AS. In fact, in some locations and seasons dust has increased (Hand et al., 2016, 2017). AN concentrations were lower than other species (Fig. 2f) and peaked in winter due to thermodynamic stability in cool weather. AN concentrations have also declined over time due to reductions in nitrogen dioxide (Lamsal et al., 2015). EC concentrations (Fig. 2g) have decreased over time (Murphy et al., 2011) and peaked in summer and early fall, similar to OM. SS concentrations were the lowest of the species shown in Fig. 2 and exhibited weak seasonality that tended to peak in spring and early summer. A shift toward higher SS concentrations occurred in 2011, related to elevated blank corrections prior to 2011 (White, 2009b).

We also examined the daily network median mass fractions, or contributions, of major species to the daily network median RCFM. Fig. 3 shows the fraction of RCFM for each species displayed in order of descending contribution. The OM mass fraction increased by nearly 10% annually over the past 12 years (XOM, Fig. 3a) and was highly seasonal, peaking strongly in late summer and fall. By mid-2016 the network median contribution of OM to RCFM was nearly 60% in summer and around 30% in winter. Contributions from AS have decreased over time by nearly 10% annually and currently are around 20–30%, a significant reduction from the ~40% in 2005 (Fig. 3b). The strong seasonality in AS mass was not evident in its mass fraction. The dust mass fraction (Fig. 3c) peaked in spring (20–30%), similar to its absolute concentrations. AN fractions were strongly seasonal with peaks in winter near 20%, decreasing to less than 5% in summer. EC fractions have also decreased over time, and although EC absolute concentrations peaked in late summer, its contribution to RCFM peaked in winter, likely related to low contributions from other species and perhaps to emissions from winter sources such as residential heating. SS was the lowest contributor (~1%) and exhibited some early spring seasonality, especially after 2011.

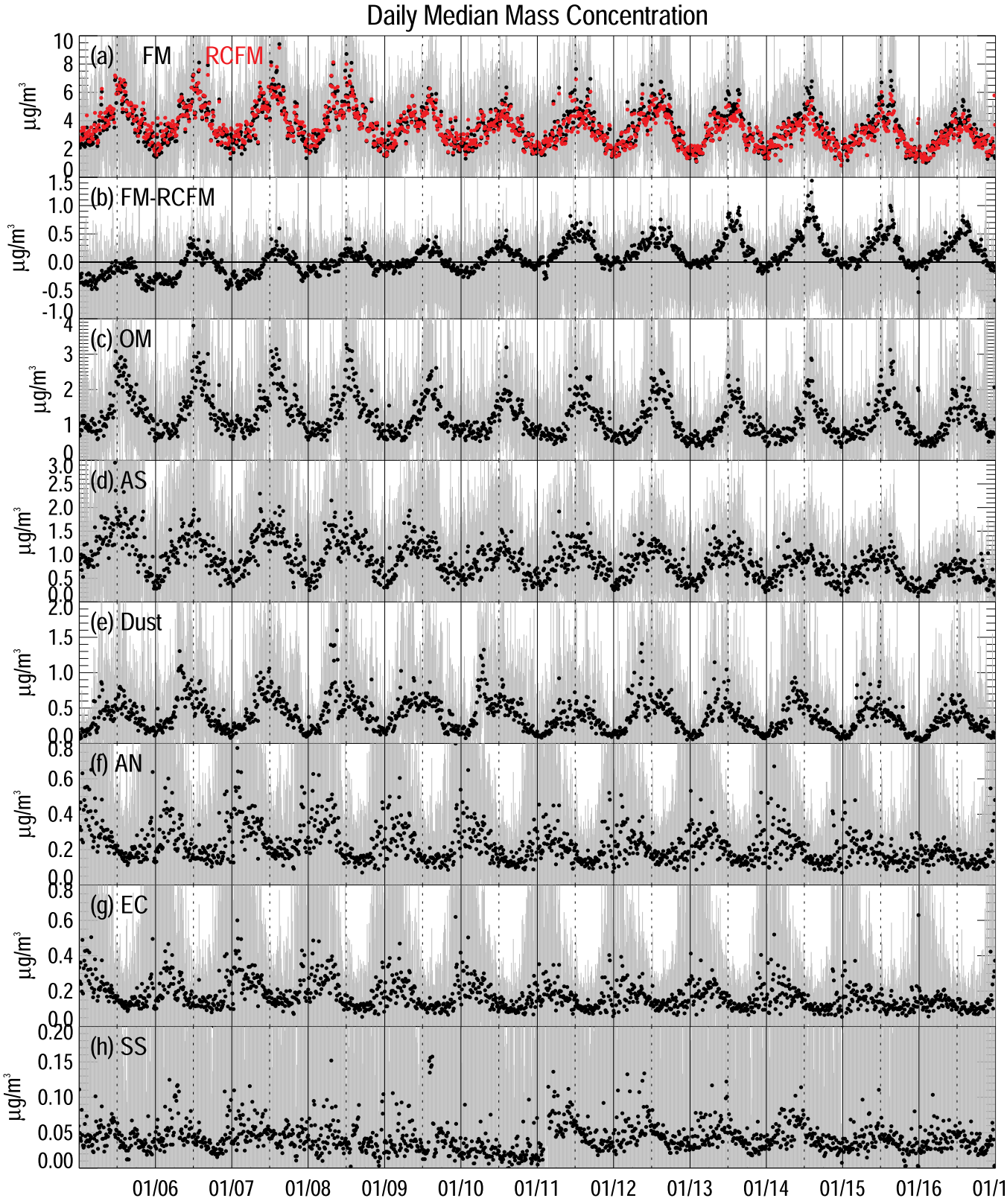

Fig. 2. IMPROVE daily network median mass concentrations for (a) $PM_{2.5}$ gravimetric mass (FM) and reconstructed fine mass (RCFM), (b) residual (FM − RCFM), (c) particulate organic matter (OM), (d) ammonium sulfate (AS), (e) fine dust, (f) ammonium nitrate (AN), (g) elemental carbon (EC), and (h) sea salt (SS). Units are µg m^{-3} and gray lines correspond to standard deviations.

As discussed in Section 2, variable RH during weighing after 2011 may have resulted in contributions of PBW to FM (not RCFM) and contributed to a larger positive residual. A "dry' residual was calculated as FM_{dry} – RCFM; a comparison of the original and dry residual is shown in Fig. 4. The original residual is plotted in red and the dry residual in black. Accounting for PBW resulted in a more negative residual and reduced the magnitude of the summer peaks, especially after 2011, but did not remove the positive trend over time.

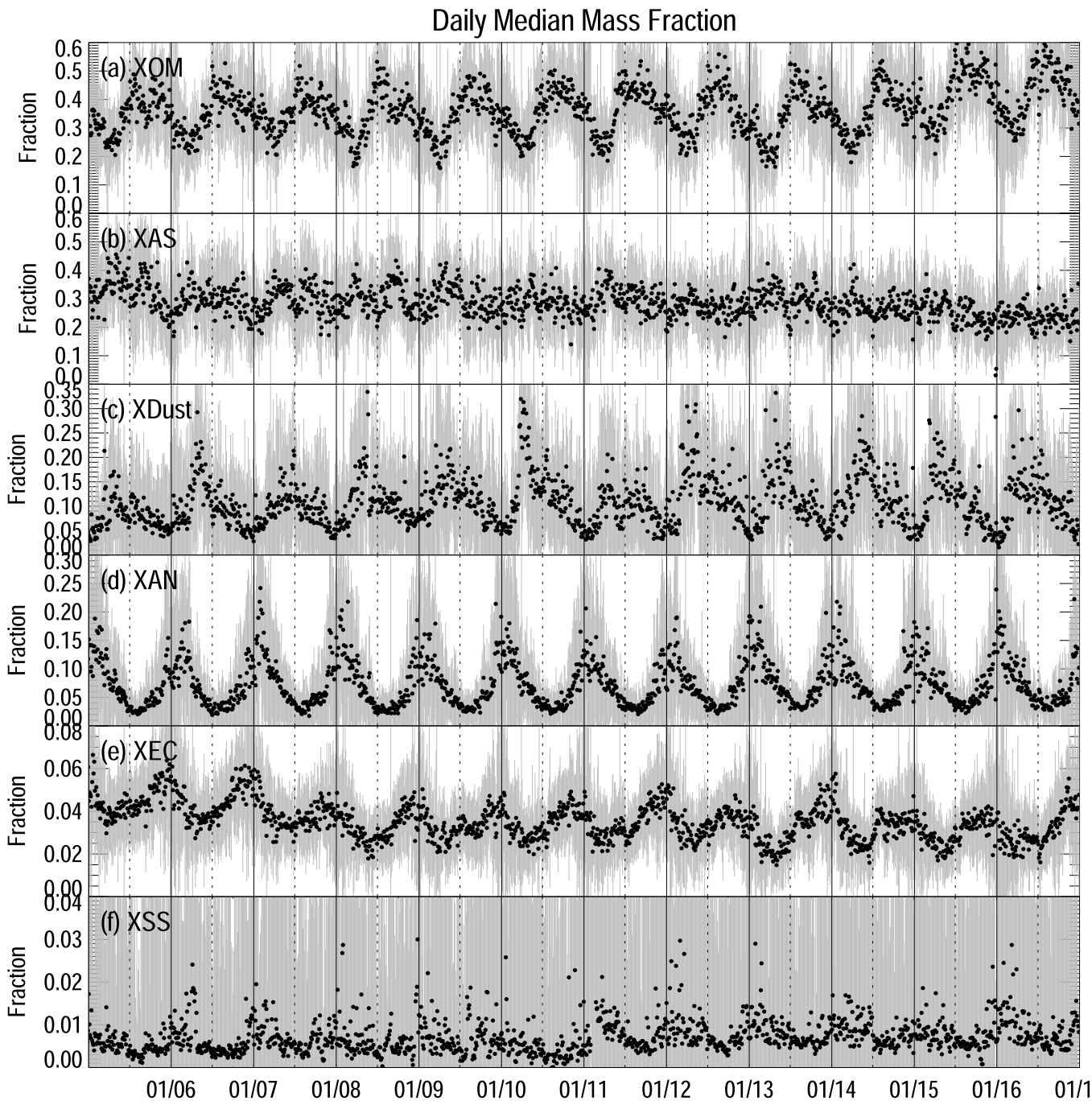

Fig. 3. IMPROVE daily network median mass fractions of reconstructed fine mass (RCFM) for (a) particulate organic matter (XOM), (b) ammonium sulfate (XAS), (c) fine dust (XDust), (d) ammonium nitrate (XAN), (e) elemental carbon (XEC), and (f) sea salt (XSS). Gray lines correspond to standard deviations.

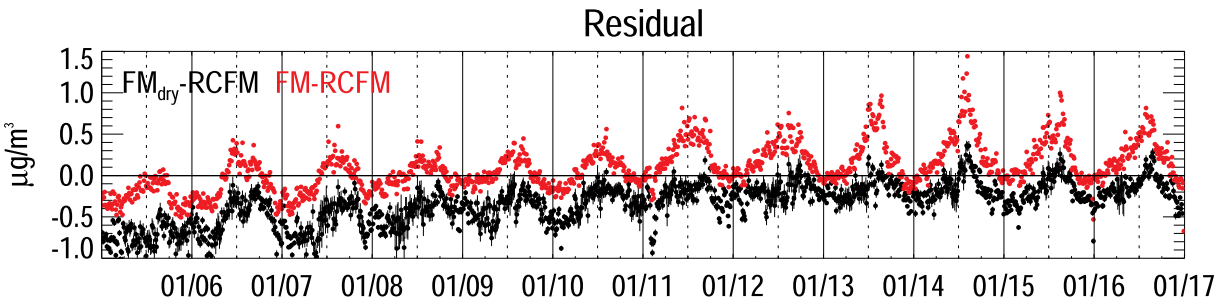

Fig. 4. IMPROVE daily network median dry residual (FM_{dry} − RCFM, μg m^{-3}) in black and original FM residual (FM − RCFM) in red. Measurement uncertainties are shown only for the dry residual.

3.2. Multiple linear regression analysis

To examine the validity of assumptions in the reconstruction algorithm over time, an MLR analysis was performed, following the methods of Malm et al. (2011) and Simon et al. (2011). A regression in the form of equation (2) was applied to daily site data for each season and each year from 2005 through 2016 with FM as the dependent variable and individual species concentrations as the independent variables:

$$FM - EC - SS = a_{AS}AS + a_{AN}AN + a_{OC}OC + a_{dust}dust \quad (2)$$

EC was not included in the regression due to collinearities with OC (Simon et al., 2011), and SS was not included due to its high relative uncertainties. Valid data were required for each species, and a 70% completeness criterion was applied for each season and year. Derived coefficients (a_{AS}, a_{AN}, a_{OC}, and a_{dust} for AS, AN, OC, and dust, respectively) from the regression are interpreted as the mass multipliers that account for unmeasured compounds, although they also include the effects of potential sampling or analytic biases. A coefficient of unity for AS, AN, and dust would suggest that the assumptions in the reconstruction algorithm were appropriate. The OC (a_{OC}) coefficient is often interpreted as the OM/OC ratio. Regional median coefficients were aggregated over four broad regions (Northwest, Northeast, Southwest, and Southeast, separated at 40° North and −100° West) and for the contiguous United States (CONUS). Temporal mean coefficients were also calculated for the two time periods shown in Fig. 1a and b (2005–2010 and 2011–2016, respectively). Regression coefficients for each species and site were considered significant for p values ≤ 0.05 and only included in spatial or temporal aggregations if they met this condition. We performed the regression using both FM and FM_{dry} as dependent variables in equation (2) to test the role of PBW on derived coefficients.

Annual CONUS network median annual and seasonal coefficients from 2005 through 2016 derived using the original FM are shown in Fig. 5 for AS (Fig. 5a), OC (Fig. 5b), and dust (Fig. 5c). AN coefficients are not shown due to volatilization from the FM filter and will not be further considered. AS coefficients were greater than one and increased over time, especially during summer and fall after 2011. These elevated values likely reflect the presence of PBW on the FM filter during weighing (Malm et al., 2011; Simon et al., 2011). Substituting FM_{dry} as the dependent variable in equation (2) resulted in AS coefficients less than one, as shown in Fig. 6a. AS coefficients appeared to increase over time but were generally within 10–20% of 1 (see Table 1). AS coefficients below one suggest that the assumption of fully neutralized SO_4^{2-} resulted in an overestimate of SO_4^{2-}-related mass or could also reflect an overestimate of PBW. The ratio of calculated hydrated AS mass to dry AS mass (AS_{wet}/AS_{dry}) at laboratory RH agreed within 10–20% on average compared to original AS coefficients (Fig. 5a), suggesting that estimates of PBW associated with SO_4^{2-} were reasonable.

While OC coefficients derived from MLR analyses are often physically interpreted as the OM/OC ratio, they may also include effects of sampling or analytical biases. Coefficients derived using FM are shown in Fig. 5b for seasonal and annual mean values. A value of 1.8 is plotted as a horizontal black line to reflect the multiplier used in the reconstruction algorithm (equation (1)). From 2005 through 2010, OC coefficients were variable over time, increased from 2011 through 2014, and then decreased in 2015 and 2016. This behavior was generally observed during all seasons but was most strongly evident in summer and fall. The increase in 2011 coincided with laboratory RH stability issues; however, OC was considered weakly hygroscopic in the calculation of PBW, and regression results obtained with FM_{dry} (Fig. 6b) suggest the amount of PBW associated with OC had very little influence on the increase in the OC coefficient after 2011.

If interpreted solely as the OM/OC ratio, the derived OC coefficients shown in Fig. 6b were consistent with other reported OM/OC values. Summer values were greater than 1.8 during the entire period and reached a value of 2.24 in 2014 before decreasing to 2.0 in 2016. These values were consistent with those reported for rural regions in the United States using a range of methods and are indicative of a more aged secondary organic aerosol (e.g., El-Zanan et al., 2005; Bae et al., 2006; Malm and Hand, 2007; Malm et al., 2011; Simon et al., 2011; Philip et al., 2014; Ruthenberg et al., 2014; Lowenthal et al., 2015; Blanchard et al., 2016). Winter values were the lowest of any season, ranging from 1.30 to 1.69 over the time period, consistent with a less aged primary organic aerosol.

Dust coefficients are shown in Figs. 5c and 6c for regressions with FM and FM_{dry}, respectively. Dust was regarded as nonhygroscopic; therefore results in Figs. 5c and 6c are similar. Coefficients were greater than one, suggesting that dust was underestimated in the reconstruction by 20–30%, consistent with previous work (Malm and Hand, 2007). Spring and summer dust coefficients were near one until they increased after 2011, which coincides with analytical changes (see Section 2). Winter, the season with the highest coefficients, also corresponded to the lowest dust concentrations.

We also investigated the spatial variability in the dry regression coefficients for sites in the broad regions of the Northwest (NW), Northeast (NE), Southwest (SW), and Southeast (SE). The regional median annual coefficients for AS, OC, and fine dust are shown in Fig. 7a, b, and 7c, respectively, and reported in Table 1. AS coefficients were lowest in the eastern regions (0.8–0.9) but gradually increased over time, suggesting that while SO_4^{2-} is still acidic, it may have become somewhat less acidic over time in the East. AS coefficients less than one suggest contributions of SO_4^{2-} to RCFM were overestimated, or PBW corrections in the East were overestimated. AS coefficients in the West were higher than in the East, although still less than one in the SW. AS coefficients were highest (near or above one) at sites in the NW. These spatial differences in AS coefficients suggest that applying a single multiplier to SO_4^{2-} in the reconstruction algorithm could contribute to under- or overestimations of SO_4^{2-} contributions to RCFM, depending on region.

The increase in OC coefficients seen for the CONUS seasonal and

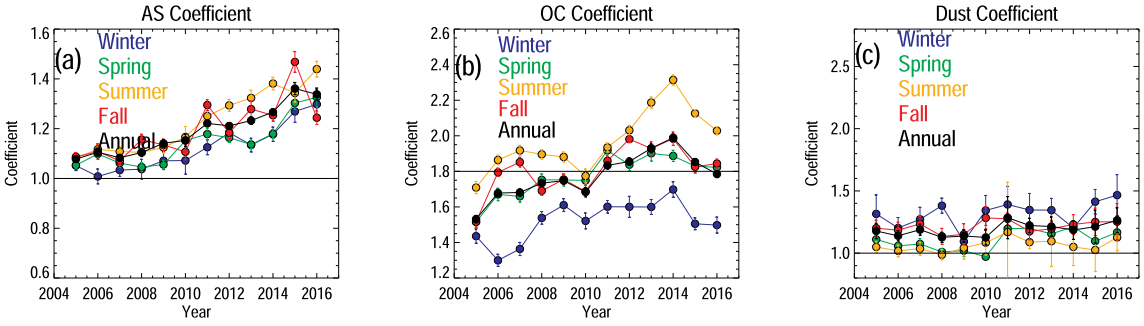

Fig. 5. IMPROVE seasonal and annual network median multiple linear regression coefficients for 2005–2016, derived using original FM for (a) ammonium sulfate (AS), (b) organic carbon (OC), and (c) fine dust. Error bars correspond to standard error.

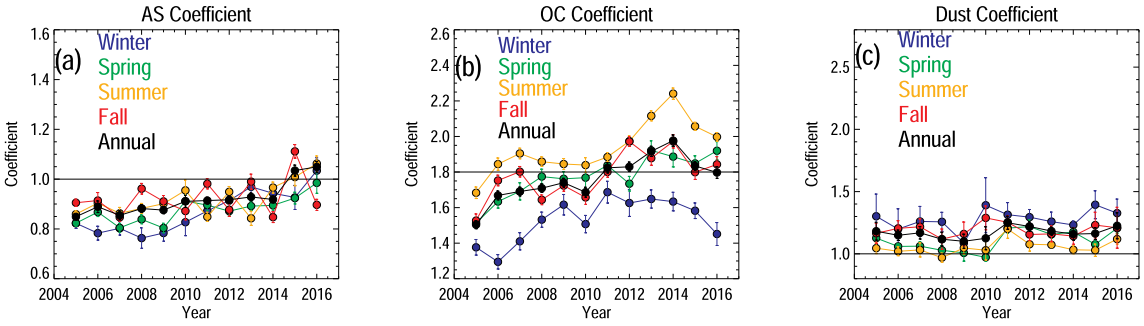

Fig. 6. IMPROVE seasonal and annual network median multiple linear regression coefficients for 2005–2016, derived using FM_{dry} for (a) ammonium sulfate (AS), (b) organic carbon (OC), and (c) fine dust. Error bars correspond to standard error.

annual results (Fig. 6b) was also evident across all of the regions (Fig. 7b). In the eastern regions, the OC coefficients were fairly stable around 1.8 until 2011, after which they reached a high value in 2014. In the western regions, the coefficients steadily increased over time from values less than 1.8 to greater than 1.8 in the NW after 2011. OC coefficients in the SW increased over time but were never greater than 1.8. These results suggest that for the NE, SE, and NW before 2011, OC contributions to RCFM were overestimated; after 2011 the contribution of OC to RCFM was underestimated. Contributions of OC to RCFM in the SW were overestimated across the time period. The sharp climb in coefficients (especially in the East) from 2011 through 2014 and their decrease in 2015 and 2016 for all regions warrant further investigation.

Dust coefficients (Fig. 7c) suggest an underestimation of dust contributions to RCFM for all regions by 20–30% but were lowest in the SW prior to 2011. The increase around 2011 for all regions is likely an analytical effect. Noisy dust coefficients for the NE region reflect the relatively low concentrations in that region.

4. Discussion

The temporal variability in the MLR coefficients presented in Fig. 6a–c points to the underlying causes for the 0.59 μg m^{-3} increase in the dry residual over the 12-year period (yearly trend of 0.05 μg m^{-3} yr^{-1}). Quantifying the relative influences of AS, OC, and dust on the dry residual requires estimates of their individual biases. To do this we defined a total dry residual bias (TB) as the difference in the dry residual and an adjusted dry residual (TB = dry residual – adjusted dry residual). The adjusted dry residual was calculated as the difference between FM_{dry} and an adjusted RCFM ($RCFM_a$). Daily $RCFM_a$ was computed by applying the regional and seasonal mean AS, OC, and dust coefficients from the two different time periods reported in Table 1 to daily SO_4^{2-}, OC, and dust data ($RCFM_a = a_{AS} \times AS + a_{OC} \times OC + a_{dust} \times dust + AN + EC + SS$). Substituting the definitions of dry residual and adjusted dry residual gives TB:

$$TB = (FM_{dry} - RCFM) - (FM_{dry} - RCFM_a) \quad (3)$$

Substituting the definition of RCFM from equation (1) and the definition of $RCFM_a$ results in equation (4):

$$TB = AS(a_{AS} - 1) + OC(a_{OC} - 1.8) + dust(a_{dust} - 1) \quad (4)$$

A negative TB suggests that RCFM was high relative to FM_{dry} (e.g., coefficients less than one) and positive TB suggests that the RCFM was low relative to FM_{dry} (e.g., coefficients greater than one). By using the form of equation (4) we can evaluate the contribution from the bias from each species explicitly to the TB.

The daily network median bias from each species and their sum (TB) are shown in Fig. 8. The figure is split into two time series to emphasize that two different sets of coefficients were applied in equation (4) for the two different time periods (2005–2010 and 2011–2016). From 2005 through 2010, the mean AS and OC biases were both negative and similar in magnitude (-0.084 μg m^{-3} and -0.076 μg m^{-3}, respectively). As seen from Fig. 8, the AS bias was generally the largest contributor to TB in spring and summer when SO_4^{2-} concentrations were largest. During this period the assumption of fully neutralized AS was an

Table 1
IMPROVE regional median multiple linear regression coefficients using FM_{dry} for 2005–2010 and 2011–2016 for ammonium sulfate (a_{AS}), organic carbon (a_{OC}) and fine dust (a_{dust}). Regions were defined by a 40° latitude and −100° longitude split. United States values correspond to CONUS sites.

Region	Northwest		Northeast		Southeast		Southwest		United States	
Years	2005–2010	2011–2016	2005–2010	2011–2016	2005–2010	2011–2016	2005–2010	2011–2016	2005–2010	2011–2016
a_{AS}										
Winter	1.05	1.13	0.73	0.82	0.73	0.82	1.03	1.14	0.80	0.94
Spring	0.85	0.96	0.83	0.85	0.81	0.89	0.90	0.94	0.84	0.91
Summer	0.95	1.11	0.88	1.01	0.87	0.92	0.91	0.84	0.89	0.95
Fall	0.99	1.03	0.88	0.97	0.87	0.94	0.93	0.91	0.90	0.95
Annual	0.94	1.06	0.83	0.94	0.81	0.90	0.95	0.96	0.88	0.96
a_{OC}										
Winter	1.46	1.60	1.59	1.79	1.56	1.75	1.20	1.38	1.46	1.60
Spring	1.61	1.78	1.73	2.01	1.85	2.01	1.61	1.67	1.69	1.86
Summer	1.80	2.01	1.93	2.13	2.06	2.21	1.69	1.98	1.83	2.05
Fall	1.69	1.88	1.68	1.88	1.82	1.99	1.58	1.79	1.68	1.88
Annual	1.64	1.84	1.73	1.96	1.80	1.99	1.57	1.72	1.67	1.86
a_{dust}										
Winter	1.51	1.46	2.34	1.93	1.44	1.93	1.15	1.23	1.25	1.30
Spring	1.08	1.20	1.17	1.35	1.11	1.15	1.00	1.17	1.04	1.17
Summer	1.05	1.06	1.37	1.40	0.91	1.03	1.04	1.12	1.02	1.09
Fall	1.20	1.23	1.53	1.99	1.22	1.19	1.16	1.18	1.19	1.19
Annual	1.17	1.24	1.53	1.67	1.18	1.15	1.08	1.18	1.14	1.20

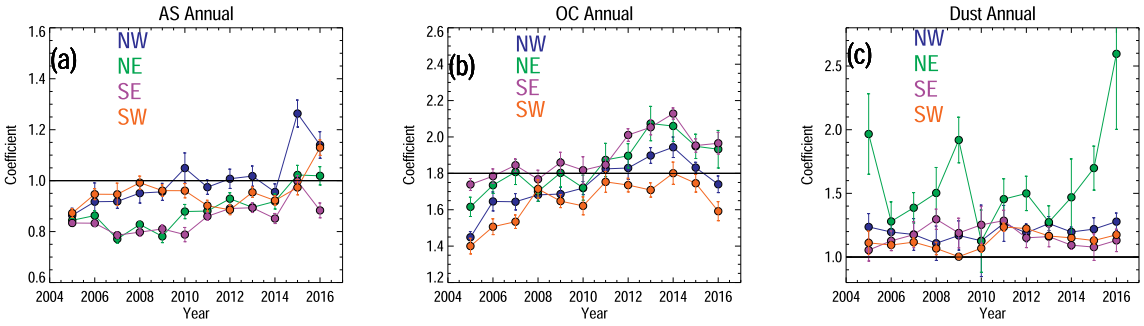

Fig. 7. IMPROVE regional, annual multiple linear regression coefficients for 2005–2016 using FM_{dry} for (a) ammonium sulfate (AS), (b) organic carbon (OC), and (c) fine dust. The Northwest (NW), Northeast (NE), Southeast (SE), and Southwest (SW) regions were defined by a 40° latitude and −100° longitude split. Error bars correspond to standard error.

overestimation. The negative OC bias contribution was greatest in winter when OM/OC values of 1.8 were likely too large in the original reconstruction algorithm (see equation (1) and Fig. 6b). The mean dust bias was positive (0.05 μg m^{-3}), consistent with underestimation of dust mass in the reconstruction algorithm. The positive contribution of dust to TB was overwhelmed by the negative AS and OC biases in the first time period.

After 2011 the TB shifted to positive, consistent with the negative dry residual and lower RCFM relative to FM_{dry}. The AS bias reduced by half and was less variable but still negative (−0.038 μg m^{-3}). The most striking change was associated with the OC bias, which increased from −0.076 μg m^{-3} to 0.057 μg m^{-3} and became the dominant contributor to the TB in summer, consistent with the high OC coefficients in summer (higher than 1.8) shown in Fig. 6b. After 2011 the positive dust bias (0.06 μg m^{-3}) accounted for most of TB in spring and part of the TB in fall.

The growing importance of OM to RCFM, OM's influence on the residual, as well as the temporal behavior of the OC coefficients raise important questions regarding OC. One is whether the increase in the OC coefficients across the network reflects real changes in the atmosphere. OC coefficients are often interpreted as OM/OC ratios, and the values derived here are in agreement with independent estimates of OM/OC from other studies and reflect previously reported seasonal and regional observations. However, it is difficult to attribute the temporal variability in the coefficients that was observed during all seasons and in all regions to changes in the atmosphere across the entire United States. Higher OM/OC ratios correspond to more aged secondary organic aerosol. These results suggest that for several years, OC became increasingly more aged and more oxygenated during all seasons and across all remote sites in the United States, followed by a reduction in OM/OC in the last couple of years of the analysis. An alternative interpretation is that the reduction of primary OC led to higher OM/OC values across the network, although this cannot explain the decrease in OM/OC values in the past two years of analysis. Perhaps other sources of carbon are being collected on the FM filter that are not characterized by the TOR analysis, such as organosulfur species (e.g., Surratt et al., 2007). However, the low concentrations of organosulfur (e.g., Froyd et al., 2010; Liao et al., 2015; Sorooshian et al., 2015) likely would not account for the mass difference and would have to be increasing across the network during all seasons. We cannot rule out the possibility that we have observed large-scale changes of OC in the atmosphere; however, the ability to test this hypothesis is limited with these data. The possible influence of analytical issues, including potential changes in sampling artifacts, on the changing coefficients must be fully explored before interpreting the changes in the OC coefficients as changes in OM/OC ratios.

It is possible that analytical contributions have influenced the temporal behavior of the OC coefficients given that similar changes occurred across the network. The temporal variability in quartz filter field blank corrections (Dillner, 2015) do not appear to account for the changes in OM/OC. Other possibilities may be due to different sampling artifacts associated with the Teflon and quartz filters. Malm et al. (2011) identified a 20% negative artifact in OC associated with the quartz filter due to sampler face velocity; however, it is unclear why these artifacts would change over time. Other issues include potential hardware degradation, hardware changes, or calibration changes. As discussed in Section 2, the TOR hardware has undergone degradations over time and recently experienced a shift to new hardware and analysis methodology. A reanalysis study of archived quartz filters, such as the study performed by Hyslop et al. (2015) for XRF filters, may help to reveal whether some of these issues could be influencing carbon data over time. While the reasons for the temporal variability in the OC coefficient are unknown, it is clear that a seasonal variability in the OC coefficients is important, and some of the bias in the residual was due to the seasonality in OM/OC ratios.

5. Conclusion

The 0.49 μg m^{-3} trend in the original FM residual (FM − RCFM) from 2005 through 2016 (0.04 μg m^{-3} yr^{-1}) in the IMPROVE network

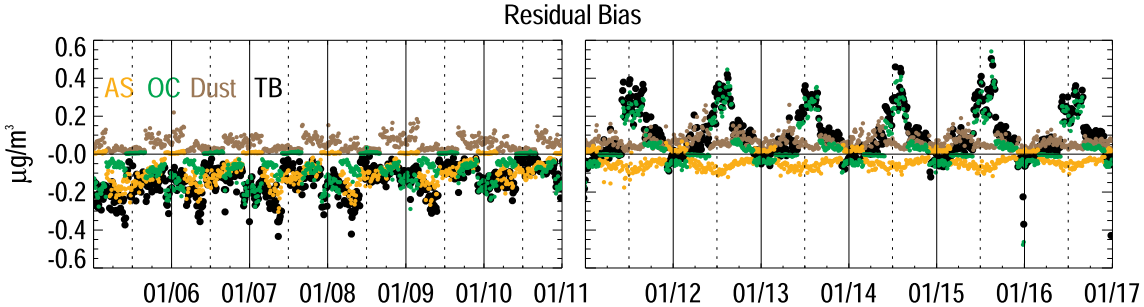

Fig. 8. IMPROVE daily network median biases for ammonium sulfate (AS), particulate organic matter (OM), and fine dust to the total dry residual bias (TB, μg m^{-3}) from 2005 through 2016. The timeline is split into two parts to reflect the different coefficients used in each period.

motivated a study to examine the assumptions in the IMPROVE reconstruction algorithm and possible changes in analytic or sampling biases. Except for summer, the residual was mostly negative before 2011 and mostly positive from 2011 through 2016. A strong seasonality was observed, with peaks in summer that intensified after 2011. An MLR approach was applied to daily and site-specific data to identify temporal, spatial, and seasonal variability in the mass multipliers assumed in the reconstruction, as well as to detect analytical and sampling biases.

We identified and corrected for the role of PBW bias on the residual through the direct estimate and subtraction of PBW from FM. This correction reduced the residual and some of the strong summer seasonality in the residual and positive biases in AS coefficients from the MLR. AS coefficients derived using FM_{dry} suggested that the assumptions of fully neutralized AS in the reconstruction algorithm were largely responsible for the negative residual, especially during summers before 2011. The magnitude of the bias may be affected by uncertainties in the PBW corrections. We also found that OC coefficients increased over time across the network until 2014 for all seasons and regions; however, values were higher in summer relative to winter and for the East relative to the West. The changes in the OC coefficients accounted for some of the temporal behavior in the residual before 2011, although the regional and seasonal variability in the OC coefficients was larger than the shifts in time. A constant OM/OC ratio of 1.8 was assumed in the original reconstruction algorithm and likely contributed to a negative bias in the residual before 2011 and to a positive residual after 2011. We have not identified the reasons for the increase in the OC coefficients that apparently occurred across the network and therefore caution the interpretation of the coefficients as OM/OC ratios. The analysis also indicated that dust was underestimated in the reconstruction algorithm and was responsible for the positive bias in spring after 2011. The analysis also revealed the possible influence of the analytical changes in 2011 on dust that warrants further investigation. Finally, while we did not further investigate the role of NO_3^- on the residual because of the noise in the MLR results, the volatilization of NO_3^- from the FM Teflon filter, as well as the form of NO_3^- assumed in reconstruction algorithm (e.g., Lee et al., 2008), also likely impacts the residual, although to a lesser degree than AS, OC, or dust due to AN's relatively lower concentrations and mass fractions.

Past regression analyses using IMPROVE data have led to recommendations for changes to the IMPROVE algorithms to reconstruct mass and light extinction coefficients (Malm and Hand, 2007; Pitchford et al., 2007). MLR analyses are useful for understanding the relative roles of species' contributions to residuals and to identify important seasonal and spatial differences. They can also help detect sampling or analytical biases that can affect data for the entire network and confound interpretations of temporal trends. Results from this analysis suggest that seasonally and regionally varying OM/OC ratios in the reconstruction algorithm would likely improve reconstructed mass and extinction estimates; however, we caution against over-interpreting these results. Assuming a more acidic form of SO_4^{2-} in the reconstruction may also reduce the bias. While analytical and sampling changes obviously must occur in a long-term network such as IMPROVE, it is important to understand the data are subject to these changes. Tuning reconstruction algorithms based on MLR results may improve comparisons between measured and RCFM and extinction, but they may only apply for the periods under which consistent analytical and sampling methodology occurred, and therefore may be accounting mostly for measurement or analysis biases rather than changing aerosol properties.

Declaration of interest

Conflicts of interest

None.

Disclaimer

This work was funded by the National Park Service Air Resources Division under cooperative agreement P14AC00728 and views presented herein are those of the authors and should not be interpreted as necessarily representing the National Park Service.

Acknowledgments

We thank David Ridley of the Massachusetts Institute of Technology for originally bringing the discrepancy between trends in measured and reconstructed fine mass to our attention. IMPROVE is a collaborative association of state, tribal, and federal agencies, and international partners. The U.S. Environmental Protection Agency is the primary funding source, with contracting and research support from the National Park Service. The Air Quality Group at the University of California, Davis, is the central analytical laboratory, with ion analysis provided by the Research Triangle Institute and carbon analysis provided by Desert Research Institute. IMPROVE data are available for download (http://vista.cira.colostate.edu/improve and http://views.cira.colostate.edu/fed). Aggregated data reported in the manuscript are available from the corresponding author.

References

Allen, H.M., Draper, D.C., Ayres, B.R., Ault, A.P., Bondy, A.L., Takahama, S., Modini, R.L., Baumann, K., Edgerton, E., Knote, C., Laskin, A., Wang, B., Fry, J.L., 2015. Influence of crustal dust and sea spray supermicron particle concentrations and acidity on inorganic NO^{3-} aerosol during the 2013 Southern Oxidant and Aerosol Study. Atmos. Chem. Phys. 15, 10669–10685. https://doi.org/10.5194/acp-15-10669-2015.

Attwood, A.R., Washenfelder, R.A., Brock, C.A., Hu, W., Baumann, K., Campuzano-Jost, P., Day, D.A., Edgerton, E.S., Murphy, D.M., Palm, B.B., McComiskey, A., Wagner, N.L., de Sa, S.S., Ortega, A., Martin, S.T., Jimenez, J.L., Brown, S.S., 2014. Trends in sulfate and organic aerosol mass in the Southeast U.S.: impact on aerosol optical depth and radiative forcing. Geophys. Res. Lett. 41, 7701–7709. https://doi.org/10.1002/2014gl061669.

Bae, M.S., Demerjian, K.L., Schwab, J.J., 2006. Seasonal estimation of organic mass to organic carbon in $PM_{2.5}$ at rural and urban locations in New York state. Atmos. Environ. 40, 7467–7479. https://doi.org/10.1016/j.atmosenv.2006.07.008.

Blanchard, C.L., Hidy, G.M., Tanenbaum, S., Edgerton, E.S., Hartsell, B.E., 2013. The Southeastern Aerosol Research and Characterization (SEARCH) study: temporal trends in gas and PM concentrations and composition, 1999-2010. J. Air Waste Manag. Assoc. 63, 247–259. https://doi.org/10.1080/10962247.2012.748523.

Blanchard, C.L., Hidy, G.M., Shaw, S., Baumann, K., Edgerton, E.S., 2016. Effects of emission reductions on organic aerosol in the southeastern United States. Atmos. Chem. Phys. 16, 215–238. https://doi.org/10.5194/acp-16-215-2016.

Carlton, A.G., Pye, H.O.T., Baker, K.R., Hennigan, C.J., 2018. Additional benefits of federal air-quality rules: model estimates of controllable biogenic secondary organic aerosol. Environ. Sci. Technol. 52, 9254–9265. https://doi.org/10.1021/acs.est.8b01869.

Chan, E.A.W., Gantt, B., McDow, S., 2018. The reduction of summer sulfate and switch from summertime to wintertime $PM_{2.5}$ concentration maxima in the United States. Atmos. Environ. 175, 25–32. https://doi.org/10.1016/j.atmosenv.2017.11.055.

Chen, L.W.A., Chow, J.C., Watson, J.G., Schichtel, B.A., 2012. Consistency of long-term elemental carbon trends from thermal and optical measurements in the IMPROVE network. Atmos. Meas. Tech. 5, 2329–2338. https://doi.org/10.5194/amt-5-2329-2012.

Cheng, X., 2015. Changes to redelivery of 1/2005 through 5/2014 data. Advisory, Doc. # da0031. http://vista.cira.colostate.edu/improve/Data/QA_QC/Advisory/da0031/da0031_2010to2014Redelivery.pdf, Accessed date: 8 October 2018.

Chow, J.C., Watson, J.G., Lowenthal, D.H., Magliano, K.L., 2005. Loss of $PM_{2.5}$ nitrate from filter samples in central California. J. Air Waste Manag. Assoc. 55, 1158–1168. https://doi.org/10.1080/10473289.2005.10464704.

Chow, J.C., Watson, J.G., Chen, L.W.A., Chang, M.C.O., Robinson, N.F., Trimble, D., Kohl, S., 2007. The IMPROVE-A temperature protocol for thermal/optical carbon analysis: maintaining consistency with a long-term database. J. Air Waste Manag. Assoc. 57, 1014–1023. https://doi.org/10.3155/1047-3289.57.9.1014.

Chow, J.C., Watson, J.G., Chen, L.W.A., Rice, J., Frank, N.H., 2010. Quantification of $PM_{2.5}$ organic carbon sampling artifacts in US networks. Atmos. Chem. Phys. 10, 5223–5239. https://doi.org/10.5194/acp-10-5223-2010.

Chow, J.C., Lowenthal, D.H., Chen, L.W.A., Wang, X.L., Watson, J.G., 2015a. Mass reconstruction methods for PM2.5: a review. Air. Qual. Atmos. Health 8, 243–263. https://doi.org/10.1007/s11869-015-0338-3.

Chow, J.C., Wang, X.L., Sumlin, B.J., Gronstal, S.B., Chen, L.W.A., Trimble, D.L., Kohl, S.D., Mayorga, S.R., Riggio, G., Hurbain, P.R., Johnson, M., Zimmermann, R., Watson, J.G., 2015b. Optical calibration and equivalence of a multiwavelength thermal/optical carbon analyzer. Aerosol Air Qual. Res. 15https://doi.org/10.4209/aaqr.2015.02.0106. 1145-+.

Dillner, A.M., 2015. Change to artifact correction method for OC carbon fraction. Advisory, Doc. # da0032. http://vista.cira.colostate.edu/improve/Data/QA_QC/Advisory/da0032/da0032_OC_artifact.pdf, Accessed date: 8 October 2018.
Dillner, A.M., Phuah, C.H., Turner, J.R., 2009. Effects of post-sampling conditions on ambient carbon aerosol filter measurements. Atmos. Environ. 43, 5937–5943. https://doi.org/10.1016/j.atmosenv.2009.08.009.
El-Zanan, H.S., Lowenthal, D.H., Zielinska, B., Chow, J.C., Kumar, N., 2005. Determination of the organic aerosol mass to organic carbon ratio in IMPROVE samples. Chemosphere 60, 485–496. https://doi.org/10.1016/j.chemosphere.2005.01.005.
Finlayson-Pitts, B.J., 2003. The trophospheric chemistry of sea salt: a molecular-level view of the chemistry of NaCl and NaBr. Chem. Rev. 103, 4801–4822.
Froyd, K.D., Murphy, S.M., Murphy, D.M., de Gouw, J.A., Eddingsaas, N.C., Wennberg, P.O., 2010. Contribution of isoprene-derived organosulfates to free tropospheric aerosol mass. Proc. Natl. Acad. Sci. 107, 21360–21365. https://doi.org/10.1073/pnas.1012561107.
Hand, J.L., Copeland, S.A., Day, D.E., Dillner, A.M., Indresand, H., Malm, W.C., McDade, C.E., Moore Jr., C.T., Pitchford, M.L., Schichtel, B.A., Watson, J.G., 2011. Spatial and Seasonal Patterns and Temporal Variability of Haze and its Constituents in the United States, IMPROVE Report V. Cooperative Institute for Research in the Atmosphere, C.S.U., Fort Collins, Colorado ISSN 0737-5352-97. http://vista.cira.colostate.edu/improve/Publications/Reports/2011/2011.htm.
Hand, J.L., Schichtel, B.A., Pitchford, M.L., Malm, W.C., Frank, N.H., 2012a. Seasonal composition of remote and urban fine particulate matter in the United States. J. Geophys. Res. 117, D05209. https://doi.org/10.1029/2011JD017122.
Hand, J.L., Schichtel, B.A., Malm, W.C., Pitchford, M.L., 2012b. Particulate sulfate ion concentration and SO_2 emission trends in the United States from the early 1990s through 2010. Atmos. Chem. Phys. 12, 10353–10365. https://doi.org/10.5194/acp-12-10353-2012.
Hand, J.L., Schichtel, B.A., Malm, W.C., Frank, N.H., 2013. Spatial and temporal trends in $PM_{2.5}$ organic and elemental carbon across the United States. Adv. Meteor., 367674. https://doi.org/10.1155/2013/367674.
Hand, J.L., White, W.H., Gebhart, K.A., Hyslop, N.P., Gill, T.E., Schichtel, B.A., 2016. Earlier onset of the spring dust season in the southwestern United States. Geophys. Res. Lett. 43, 4001–4009. https://doi.org/10.1002/2016GL068519.
Hand, J.L., Gill, T.E., Schichtel, B.A., 2017. Spatial and seasonal variability in fine mineral dust and coarse aerosol mass at remote sites across the United States. J. Geophys. Res. Atmos. 122, 3080–3097. https://doi.org/10.1002/2016jd026290.
Hering, S., Cass, G., 1999. The magnitude of bias in the measurement of $PM_{2.5}$ arising from volatilization of particulate nitrate from teflon filters. J. Air Waste Manag. Assoc. 49, 725–733. https://doi.org/10.1080/10473289.1999.10463843.
Hidy, G.M., Blanchard, C.L., Baumann, K., Edgerton, E., Tanenbaum, S., Shaw, S., Knipping, E., Tombach, I., Jansen, J., Walters, J., 2014. Chemical climatology of the southeastern United States, 1999-2013. Atmos. Chem. Phys. 14, 11893–11914. https://doi.org/10.5194/acp-14-11893-2014.
Hyslop, N.P., White, W.H., 2009. Estimating precision using duplicate measurements. J. Air Waste Manag. Assoc. 59, 1032–1039. https://doi.org/10.3155/1047-3289.59.9.1032.
Hyslop, N.P., Trzepla, K., White, W.H., 2015. Assessing the suitability of historical $PM_{2.5}$ element measurements for trend analysis. Environ. Sci. Technol. 49, 9247–9255. https://doi.org/10.1021/acs.est.5b01572.
Indresand, H., Dillner, A.M., 2012. Experimental characterization of sulfur interference in IMPROVE aluminum and silicon XRF data. Atmos. Environ. 61, 140–147. https://doi.org/10.1016/j.atmosenv.2012.06.079.
Isaaks, E.H., Mohan Srivastava, R., 1989. An Introduction to Applied Geostatistics. Oxford University Press, New York ISBN: 978-0195050134.
Jimenez, J.L., Canagaratna, M.R., Donahue, N.M., Prevot, A.S.H., Zhang, Q., Kroll, J.H., DeCarlo, P.F., Allan, J.D., Coe, H., Ng, N.L., Aiken, A.C., Docherty, K.S., Ulbrich, I.M., Grieshop, A.P., Robinson, A.L., Duplissy, J., Smith, J.D., Wilson, K.R., Lanz, V.A., Hueglin, C., Sun, Y.L., Tian, J., Laaksonen, A., Raatikainen, T., Rautiainen, J., Vaattovaara, P., Ehn, M., Kulmala, M., Tomlinson, J.M., Collins, D.R., Cubison, M.J., Dunlea, E.J., Huffman, J.A., Onasch, T.B., Alfarra, M.R., Williams, P.I., Bower, K., Kondo, Y., Schneider, J., Drewnick, F., Borrmann, S., Weimer, S., Demerjian, K., Salcedo, D., Cottrell, L., Griffin, R., Takami, A., Miyoshi, T., Hatakeyama, S., Shimono, A., Sun, J.Y., Zhang, Y.M., Dzepina, K., Kimmel, J.R., Sueper, D., Jayne, J.T., Herndon, S.C., Trimborn, A.M., Williams, L.R., Wood, E.C., Middlebrook, A.M., Kolb, C.E., Baltensperger, U., Worsnop, D.R., 2009. Evolution of organic aerosols in the atmosphere. Science 326 (5959), 1525–1529. https://doi.org/10.1126/science.1180353.
Kaku, K.C., Reid, J.S., Hand, J.L., Edgerton, E.S., Holben, B.N., Zhange, J., Holz, R.E., 2018. Assessing the challenges of surface-level aerosol mass estimates from remote sensing during the SEAC4RS and SEARCH campaigns: baseline surface observations and remote sensing in the southeastern United States. J. Geophys. Res. Atmos. 123 (14), 7530–7562. https://doi.org/10.1029/2017JD028074.
Kim, P.S., Jacob, D.J., Fisher, J.A., Travis, K., Yu, K., Zhu, L., Yantosca, R.M., Sulprizio, M.P., Jimenez, J.L., Campuzano-Jost, P., Froyd, K.D., Liao, J., Hair, J.W., Fenn, M.A., Butler, C.F., Wagner, N.L., Gordon, T.D., Welti, A., Wennberg, P.O., Crounse, J.D., St Clair, J.M., Teng, A.P., Millet, D.B., Schwarz, J.P., Markovic, M.Z., Perring, A.E., 2015. Sources, seasonality, and trends of southeast US aerosol: an integrated analysis of surface, aircraft, and satellite observations with the GEOS-Chem chemical transport model. Atmos. Chem. Phys. 15, 10411–10433. https://doi.org/10.5194/acp-15-10411-2015.
Lamsal, L.N., Duncan, B.N., Yoshida, Y., Krotkov, N.A., Pickering, K.E., Streets, D.G., Lu, Z.F., 2015. U.S. NO_2 trends (2005-2013): EPA air quality system (AQS) data versus improved observations from the ozone monitoring instrument (OMI). Atmos. Environ. 110, 130–143. https://doi.org/10.1016/j.atmosenv.2015.03.055.
Lee, T., Yu, X.Y., Ayres, B., Kreidenweis, S.M., Malm, W.C., Collett Jr., J.L., 2008. Observations of fine and coarse particle nitrate at several rural locations in the United States. Atmos. Environ. 42, 2720–2732. https://doi.org/10.1016/j.atmosenv.2007.05.016.
Liao, J., Froyd, K.D., Murphy, D.M., Keutsch, F.N., Yu, G., Wennberg, P.O., St Clair, J.M., Crounse, J.D., Wisthaler, A., Mikoviny, T., Jimenez, J.L., Campuzano-Jost, P., Day, D.A., Hu, W.W., Ryerson, T.B., Pollack, I.B., Peischl, J., Anderson, B.E., Ziemba, L.D., Blake, D.R., Meinardi, S., Diskin, G., 2015. Airborne measurements of organosulfates over the continental US. J. Geophys. Res. Atmos. 120, 2990–3005. https://doi.org/10.1002/2014jd022378.
Lowenthal, D.H., Kumar, N., 2003. $PM_{2.5}$ mass and light extinction reconstruction in IMPROVE. J. Air Waste Manag. Assoc. 53, 1109–1120. https://doi.org/10.1080/10473289.2003.10466264.
Lowenthal, D., Kumar, N., 2006. Light scattering from sea-salt aerosols at interagency monitoring of protected visual environments (IMPROVE) sites. J. Air Waste Manag. Assoc. 56, 636–642. https://doi.org/10.1080/10473289.2006.10464478.
Lowenthal, D., Zielinska, B., Samburova, V., Collins, D., Taylor, N., Kumar, N., 2015. Evaluation of assumptions for estimating chemical light extinction at US national parks. J. Air Waste Manag. Assoc. 65 (3), 249–260. https://doi.org/10.1080/10962247.2014.986307.
Malm, W.C., Hand, J.L., 2007. An examination of aerosol physical and optical properties of aerosols collected in the IMPROVE Program. Atmos. Environ. 41, 3407–3427. https://doi.org/10.1016/j.atmosenv.2006.12.012.
Malm, W.C., Sisler, J.F., Huffman, D., Eldred, R.A., Cahill, T.A., 1994. Spatial and seasonal trends in particle concentration and optical extinction in the United States. J. Geophy. Res > 99 (D1), 1347–1370. https://doi.org/10.1029/93JD02916.
Malm, W.C., Schichtel, B.A., Pitchford, M.L., 2011. Uncertainties in $PM_{2.5}$ gravimetric and speciation measurements and what we can learn from them. J. Air Waste Manage. Assoc. 61, 1131–1149. https://doi.org/10.1080/10473289.2001.603998. special Xi'an issue.
Malm, W.C., Schichtel, B.A., Hand, J.L., Collett, J.L., 2017. Concurrent temporal and spatial trends in sulfate and organic mass concentrations measured in the IMPROVE monitoring program. J. Geophys. Res. Atmos. 122, 10341–10355. https://doi.org/10.1002/2017jd026865.
McDade, C., 2007. Diminished wintertime nitrate concentrations in late 1990s. Advisory, Doc. # da0002. http://vista.cira.colostate.edu/improve/Data/QA_QC/Advisory/da0002/da0002_WinterNO3.pdf, Accessed date: 8 October 2018.
Murphy, D.M., Chow, J.C., Leibensperger, E.M., Malm, W.C., Pitchford, M., Schichtel, B.A., Watson, J.G., White, W.H., 2011. Decreases in elemental carbon and fine particle mass in the United States. Atmos. Chem. Phys. 11, 4679–4686. https://doi.org/10.5194/acp-11-4679-2011.
Perrino, C., Catrambone, M., Farao, C., Canepari, S., 2016. Assessing the contribution of water to the mass closure of PM10. Atmos. Environ. 140, 555–564. https://doi.org/10.1016/j.atmosenv.2016.06.038.
Philip, S., Martin, R.V., Pierce, J.R., Jimenez, J.L., Zhang, Q., Canagaratna, M.R., Spracklen, D.V., Nowlan, C.R., Lamsal, L.N., Cooper, M.J., Krotkov, N.A., 2014. Spatially and seasonally resolved estimate of the ratio of organic mass to organic carbon. Atmos. Environ. 87, 34–40. https://doi.org/10.1016/j.atmosenv.2013.11.065.
Pitchford, M.L., Malm, W.C., Schichtel, B.A., Kumar, N., Lowenthal, D., Hand, J.L., 2007. Revised algorithm for estimating light extinction from IMPROVE particle speciation data. J. Air Waste Manag. Assoc. 57, 1326–1336. https://doi.org/10.3155/1047-3289.57.11.1326.
Prenni, A.J., Petters, M.D., Kreidenweis, S.M., DeMott, P.J., Ziemann, P.J., 2007. Cloud droplet activation of secondary organic aerosol. J. Geophys. Res. Atmos. 112. https://doi.org/10.1029/2006jd007963.
Prenni, A.J., Day, D.E., Evanoski-Cole, A.R., Sive, B.C., Hecobian, A., Zhou, Y., Gebhart, K.A., Hand, J.L., Sullivan, A.P., Li, Y., Schurman, M.I., Desyaterik, Y., Malm, W.C., Collett, J.L., Schichtel, B.A., 2016. Oil and gas impacts on air quality in federal lands in the Bakken region: an overview of the Bakken Air Quality Study and first results. Atmos. Chem. Phys. 16, 1401–1416. https://doi.org/10.5194/acp-16-1401-2016.
Rees, S.L., Robinson, A.L., Khlystov, A., Stanier, C.O., Pandis, S.N., 2004. Mass balance closure and the federal reference method for $PM_{2.5}$ in Pittsburgh, Pennsylvania. Atmos. Environ. 38, 3305–3318. https://doi.org/10.1016/j.atmosenv.2004.03.016.
Ridley, D.A., Heald, C.L., Ridley, K.J., Kroll, J.H., 2018. Causes and consequences of decreasing atmospheric organic aerosol in the United States. Proc. Natl. Acad. Sci. 115, 290–295. https://doi.org/10.1073/pnas.1700387115.
Ruthenburg, T.C., Perlin, P.C., Liu, V., McDade, C.E., Dillner, A.M., 2014. Determination of organic matter and organic matter to organic carbon ratios by infrared spectroscopy with application to selected sites in the IMPROVE network. Atmos. Environ. 86, 47–57. https://doi.org/10.1016/j.atmosenv.2013.12.034.
Schichtel, B.A., Hand, J.L., Barna, M.G., Gebhart, K.A., Copeland, S., Vimont, J., Malm, W.C., 2017. Origin of fine particulate carbon in the rural United States. Environ. Sci. Technol. 51, 9846–9855. https://doi.org/10.1021/acs.est.7b00645.
Shah, V., Jaegle, L., Thornton, J.A., Lopez-Hilfiker, F.D., Lee, B.H., Schroder, J.C., Campuzano-Jost, P., Jimenez, J.L., Guo, H.Y., Sullivan, A.P., Weber, R.J., Green, J.R., Fiddler, M.N., Bililign, S., Campos, T.L., Stell, M., Weinheimer, A.J., Montzka, D.D., Brown, S.S., 2018. Chemical feedbacks weaken the wintertime response of particulate sulfate and nitrate to emissions reductions over the eastern United States. Proc. Natl. Acad. Sci. 115 (32), 8110–8115. https://doi.org/10.1073/pnas.1803295115.
Silvern, R.F., Jacob, D.J., Kim, P.S., Marais, E.A., Turner, J.R., Campuzano-Jost, P., Jimenez, J.L., 2017. Inconsistency of ammonium-sulfate aerosol ratios with thermodynamic models in the eastern US: a possible role of organic aerosol. Atmos. Chem. Phys. 17, 5107–5118. https://doi.org/10.5194/acp-17-5107-2017.
Simon, H., Bhave, P.V., Swall, J.L., Frank, N.H., Malm, W.C., 2011. Determining the spatial and seasonal variability in OM/OC ratios across the US using multiple

regression. Atmos. Chem. Phys. 11, 2933–2949. https://doi.org/10.5194/acp-11-2933-2011.

Solomon, P.A., Crumpler, D., Flanagan, J.B., Jayanty, R.K.M., Rickman, E.E., McDade, C.E., 2014. US national $PM_{2.5}$ chemical speciation monitoring networks-CSN and IMPROVE: description of networks. J. Air Waste Manag. Assoc. 64 (12), 1410–1438. https://doi.org/10.1080/10962247.2014.956904.

Sorooshian, A., Crosbie, E., Maudlin, L.C., Youn, J.S., Wang, Z., Shingler, T., Ortega, A.M., Hersey, S., Woods, R.K., 2015. Surface and airborne measurements of organosulfur and methanesulfonate over the western United States and coastal areas. J. Geophys. Res. Atmos. 120, 8535–8548. https://doi.org/10.1002/2015jd023822.

Surratt, J.D., Kroll, J.H., Kleindienst, T.E., Edney, E.O., Claeys, M., Sorooshian, A., Ng, N.L., Offenberg, J.H., Lewandowski, M., Jaoui, M., Flagan, R.C., Seinfeld, J.H., 2007. Evidence for organosulfates in secondary organic aerosol. Environ. Sci. Technol. 41, 517–527. https://doi.org/10.1021/es062081q.

Theil, H., 1950. A rank-invariant method of linear and polynomial regression analysis. Proc. Kon. Ned. Akad. v Wetensch., A. 53, 386–392. https://doi.org/10.1007/978-94-011-2546-8_20. 521-525, 1397-1412.

Turpin, B.J., Lim, H.J., 2001. Species contributions to $PM_{2.5}$ mass concentrations: revisiting common assumptions for estimating organic mass. Aerosol Sci. Technol. 35, 602–610. https://doi.org/10.1080/02786820152051454.

U.S. EPA, 2003. Guidance for Tracking Progress under the Regional Haze Rule, EPA-454/B-03-004. U.S. Environmental Protection Agency, Research Triangle Park, North Carolina. http://www.epa.gov/ttnamti1/files/ambient/visible/tracking.pdf, Accessed date: 8 October 2018.

U.S. EPA, 2016. Quality Assurance Guidance Document 2.12: Monitoring $PM_{2.5}$ in Ambient Air Using Designated Reference or Class I Equivalent Methods, EPA-454/B-16-001. U.S. Environmental Protection Agency, Research Triangle Park, North Carolina. https://www3.epa.gov/ttnamti1/files/ambient/pm25/qa/m212.pdf, Accessed date: 8 October 2018.

Watson, J.G., Chow, J.C., Chen, L.W.A., Frank, N.H., 2009. Methods to assess carbonaceous aerosol sampling artifacts for IMPROVE and other long-term networks. J. Air Waste Manag. Assoc. 59, 898–911. https://doi.org/10.3155/1047-3289.59.8.898.

Weber, R.J., Guo, H.Y., Russell, A.G., Nenes, A., 2016. High aerosol acidity despite declining atmospheric sulfate concentrations over the past 15 years. Nat. Geosci. 9https://doi.org/10.1038/ngeo2665. 282-+.

Wexler, A.S., Clegg, S.L., 2002. Atmospheric aerosol models for systems including the ions H+, NH4+, Na+, SO42-, NO3-,Cl-, Br-, and H2O. J. Geophys. Res. Atmos. 107. https://doi.org/10.1029/2001jd000451.

White, W.H., 2006a. Elemental concentrations of Al above the MDL can go undetected, Advisory, Doc. # da0010. http://vista.cira.colostate.edu/improve/Data/QA_QC/Advisory/da0010/da0010_Almdl.pdf, Accessed date: 8 October 2018.

White, W.H., 2006b. S interference in XRF determination of Si, Advisory, Doc. # da0011. http://vista.cira.colostate.edu/improve/Data/QA_QC/Advisory/da0011/da0011_S_Si.pdf, Accessed date: 8 October 2018.

White, W.H., 2007. Shift in EC/OC split with 1 January 2005 TOR hardware upgrade, Advisory, Doc. # da0016. http://vista.cira.colostate.edu/improve/Data/QA_QC/Advisory/da0016/da0016_TOR2005.pdf, Accessed date: 8 October 2018.

White, W.H., 2008. Chemical markers for sea salt in IMPROVE aerosol data. Atmos. Environ. 42, 261–274. https://doi.org/10.1016/j.atmosenv.2007.09.040.

White, W.H., 2009a. Inconstant bias in XRS sulfur- Advisory update to da0012, Advisory, Doc. # da0023. http://vista.cira.colostate.edu/improve/Data/QA_QC/Advisory/da0023/da0023_DA_SSO4_update.pdf, Accessed date: 8 October 2018.

White, W.H., 2009b. Under-correction of chloride concentrations for filter blank levels – historical advisory: applies to downloads before 11/23/2009, Advisory, Doc. # da0024. http://vista.cira.colostate.edu/improve/Data/QA_QC/Advisory/da0024/da0024_HDA_Chloride.pdf, Accessed date: 8 October 2018.

White, W.H., 2016. Increased variation of humidity in the weighing laboratory, Advisory, Doc. # da0035. http://vista.cira.colostate.edu/improve/Data/QA_QC/Advisory/da0035/da0035_IncreasedRH.pdf, Accessed date: 8 October 2018.

White, W.H., 2017. Negative chloride concentrations at salt-poor sites, Advisory, Doc. # da0036. http://vista.cira.colostate.edu/improve/Data/QA_QC/Advisory/da0036/da0036_chloride_loss.pdf, Accessed date: 8 October 2018.

Xu, L., Guo, H.Y., Boyd, C.M., Klein, M., Bougiatioti, A., Cerully, K.M., Hite, J.R., Isaacman-VanWertz, G., Kreisberg, N.M., Knote, C., Olson, K., Koss, A., Goldstein, A.H., Hering, S.V., de Gouw, J., Baumann, K., Lee, S.H., Nenes, A., Weber, R.J., Ng, N.L., 2015. Effects of anthropogenic emissions on aerosol formation from isoprene and monoterpenes in the southeastern United States. Proc. Natl. Acad. Sci. 112 (1), 37–42. https://doi.org/10.1073/pnas.1417609112.

Zhang, X., 2017. UCD IMPROVE Standard Operating Procedure #351: Data Processing and Validation. SOP. http://vista.cira.colostate.edu/improve/wp-content/uploads/2018/01/IMPROVE-SOP-351_Data-Processing-and-Validation_12.2017_updated.pdf, Accessed date: 8 October 2018.